Electronic Supporting Information

Regulating structural asymmetry via fluorination engineering in hybrid lead bromide perovskites

Hua-Yang Ru, [a] Zhao-Yang Wang, [a] Hua-Li Liu, * [a] and Shuang-Quan Zang * [a]

[a]*Henan Key Laboratory of Crystalline Molecular Functional Materials, Green Catalysis Center, and College of Chemistry, Zhengzhou University, Zhengzhou 450001, China.*

Experimental section

Materials and reagents

All reagents and solvents were used directly as received without further purification. Isopropylamine hydrochloride (97%), (*R*)-1,1,1-trifluoropropan-2-amine hydrochloride (98%) and (*S*)-1,1,1-trifluoropropan-2-amine hydrochloride were purchased from Leyan reagent. Lead(II) bromide ($PbBr_2$), and hydrobromic acid (HBr, 48 wt.% in H_2O), methanol (CH_3OH, AR) were purchased from Energy Chemical.

Synthesis

Preparation of 1*R*/2*S* and $(C_3H_{10}N)_3PbBr_5$ single crystals.

1*R*/2*S* or $(C_3H_{10}N)_3PbBr_5$ were prepared with stoichiometric quantities of $PbBr_2$·(0.2 mmol, 0.074 g) and (*R*)-/(*S*)-1,1,1-trifluoropropan-2-amine hydrochloride (0.2 mmol, 0.030 g) or isopropylamine hydrochloride (0.2 mmol, 0.019 g) in mixed solution of HBr (1 mL) and CH_3OH (1 mL). A clear solution was afforded by heating the mixture at 130 °C and stirring for 20 min. And the crystals of **1*R*/2*S*** or $(C_3H_{10}N)_3PbBr_5$ were obtained at room temperature overnight. The crystals were washed with cold diethyl ether and dried under vacuum at 60 °C for 2 h. (Yield: 72%)

Fabrication of chiral thin films.

Quartz substrates (1.5×1.5 cm^2) were washed by ethanol, acetone and deionized water in the ultrasonic cleaner for 10 min, respectively. Then, the substrates were treated in a plasma-cleaner with oxygen plasma to improve the surface wettability. To prepare chiral thin films, **1*R*/2*S*** or $(C_3H_{10}N)_3PbBr_5$ were dissolved in 0.1 mL DMF with a specific concentration (20 wt%) as the precursor solution. Subsequently, the resultant precursor solution was spin-coated on the quartz substrate at a speed of 3000 rpm for 30 s, followed by annealing at 60 °C for 10 min on a hot plate to induce crystallization. Spin-coating and annealing were performed in the N_2-filled glove box.

Characterization

Powder X-ray Diffraction (PXRD) patterns of the samples were recorded on a D/MAX-3D diffractometer (Cu Kα, λ = 1.5418 Å). Simulated powder patterns were obtained with Mercury software and crystallographic information file (CIF) from a single crystal X-ray experiment. Steady-state photoluminescence (PL) spectroscopy were carried out with a HORIBA FluoroLog-3 fluorescence spectrometer. Luminescence lifetimes were performed on a HORIBA FluoroLog-3 fluorescence spectrometer that was equipped with a 370 nm-laser and was operating in time-correlated single-photon counting (TCSPC) mode. The photoluminescence quantum yields PLQYs were measured using an integrating sphere on a HORIBA Scientific Fluorolog-3 spectrofluorometer. UV-vis absorption spectra were obtained by means of a Hitachi UH4150 UV-visible spectrophotometer. (FTIR-ATR) spectra were conducted in the range of 500-4000 cm^{-1} on a Bruker ALPHA spectrometer. The Raman spectra were recorded on labRAM HR Evolution-HORIBA Raman system equipped with a CCD detector using a 532 nm He-Cd laser as the excitation source. Circular dichroism (CD) spectra were recorded on a Chirascan V100 spectropolarimeter. Circularly polarized luminescence (CPL) spectra were measured on a JASCO CPL-300.

Single-crystal X-ray diffraction Analysis.

The diffraction data of **1*R*/2*S*** and $(C_3H_{10}N)_3PbBr_5$ were collected on a Rigaku XtaLAB Pro diffractometer with Cu-Kα radiation (λ = 1.54184 Å) at 200 K. Data collection and reduction were

performed using the program CrysAlisPro.[1] The crystal structures were solved with direct methods (SHELXS)[2] and refined by full-matrix least squares on F^2 using OLEX2,[3] which utilizes the SHELXL-2015 module.[4] The imposed restraints in least-squares refinement of each structure were noted in the corresponding CIF files. Thus only a general description of the structural refinement strategy is presented here. All non-hydrogen atoms were refined anisotropically. Hydrogen atoms were placed in calculated positions refined using idealized geometries and assigned fixed isotropic displacement parameters. Detailed information about the X-ray crystal data, intensity collection procedure, and refinement results for all organic-inorganic hybrid perovskites compounds is summarized in Table S1 and Table S8.

Theoretical calculation.

We have employed the Vienna Ab initio Simulation Package (VASP)[5, 6] to perform all density functional theory (DFT) calculations within spin-polarized frame. The elemental core and valence electrons were represented by the projector augmented wave (PAW) method and plane-wave basis functions with a cutoff energy of 400 eV. Generalized gradient approximation with the Perdew-Burke-Ernzerhof (GGA-PBE) exchange-correlation functional was employed in the calculations.[7] Geometry optimizations were performed with the force convergency smaller than 0.05 eV/Å. The DFT-D3 empirical correction method was employed to describe van der Waals interactions.[8, 9] The original bulk structures of **1*R***, **2*S*** and $(C_3H_{10}N)_3PbBr_5$ have been optimized before the construction of surfaces with the Monkhorst-Pack k-point of 3×2×1, 1×2×3 and 3×2×1, respectively. The formation and dissociation energies are defined as:

$$\Delta E_{fe}=[E(\text{total})-E(\text{reference})]/\mu$$

E(total) is the total energy of **1*R*** or **2*S*** or $(C_3H_{10}N)_3PbBr_5$. μ is the number of atoms in the cell. E(reference) is the energy of the $H_7C_3NF_3$, $H_{10}C_3N$ molecule in the gas phase and the energy of Pb bulk, $PbBr_2$ bulk, graphite.

Supporting Figures

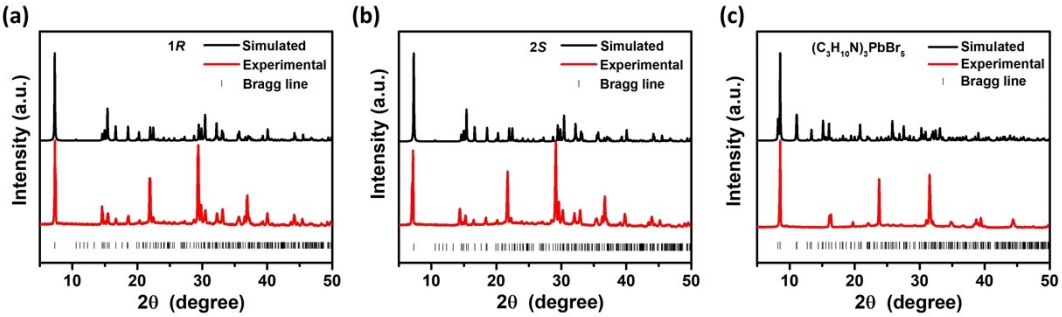

Fig. S1 Powder X-ray diffraction patterns of (a) **1*R***, (b) **2*S*** and (c) $(C_3H_{10}N)_3PbBr_5$.

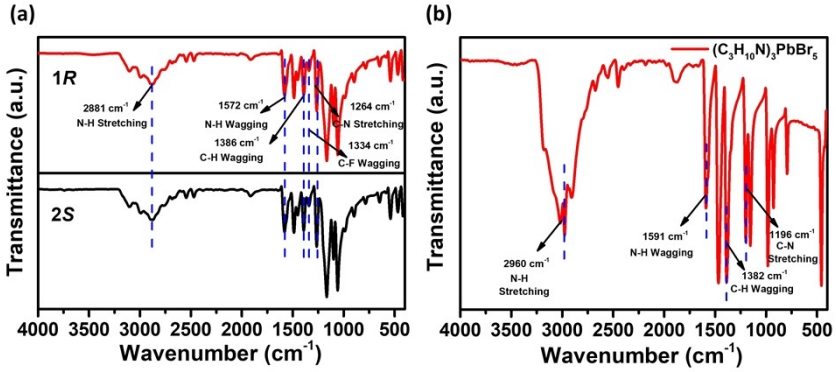

Fig. S2 FTIR spectra of (a) **1*R*/2*S*** and (b) $(C_3H_{10}N)_3PbBr_5$ powders. The vibrational frequencies at 2881 and 1572 cm^{-1} in **1*R*/2*S***, 2960 and 1591 cm^{-1} in $(C_3H_{10}N)_3PbBr_5$, assigned to the stretching and wagging modes of the N-H bonds, respectively. The peaks located at 1386 and 1264 cm^{-1} in **1*R*/2*S***, 1382 and 1196 cm^{-1} in $(C_3H_{10}N)_3PbBr_5$ were attributed to the stretching modes of C-H and C-N bonds. The vibration peaks at 1334 cm^{-1} is attributed to the wagging mode of the C-F bonds in **1*R*/2*S***.

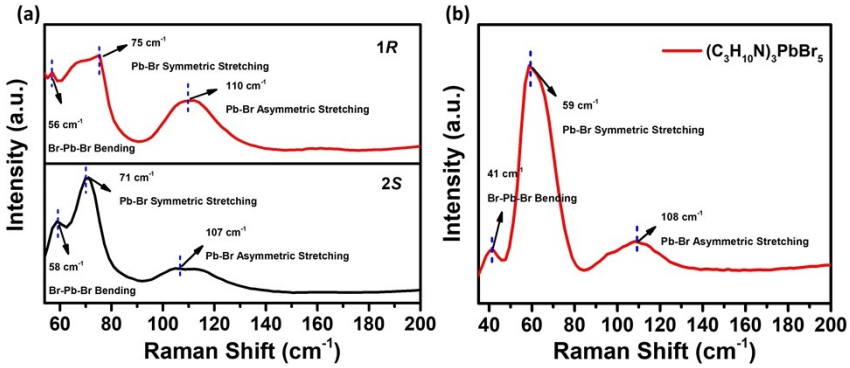

Fig. S3 Raman spectra of (a) **1*R*/2*S*** and (b) $(C_3H_{10}N)_3PbBr_5$ crystals recorded at room temperature. The observed bands at about 56, 75 and 110 cm^{-1} at **1*R*/2*S*** , 41, 59 and 108 cm^{-1} at $(C_3H_{10}N)_3PbBr_5$, correspond to the bending mode of Br-Pb-Br bond, symmetric and asymmetric stretching mode of Pb-Br bond.

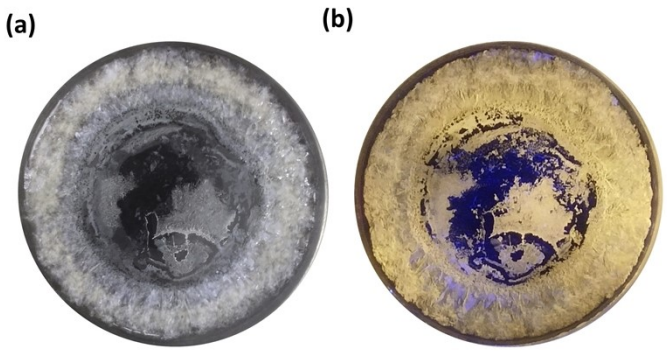

Fig. S4 (a) Optical image and (b) fluorescent image of **1*R*** under UV light (365 nm).

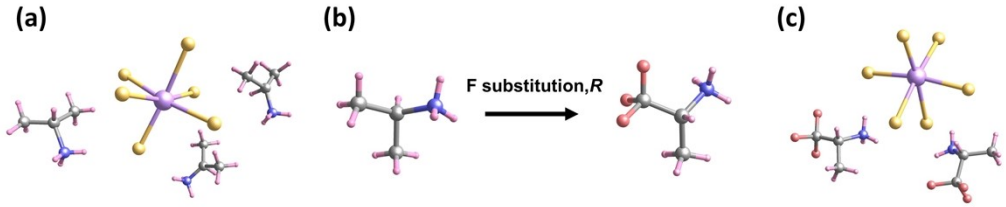

Fig. S5 The illustration of asymmetry unit of (a) $(C_3H_{10}N)_3PbBr_5$ and (c) **1*R***. (b) Schematic structure of achiral ligand (left side) and F-substituted chiral ligand (right side).

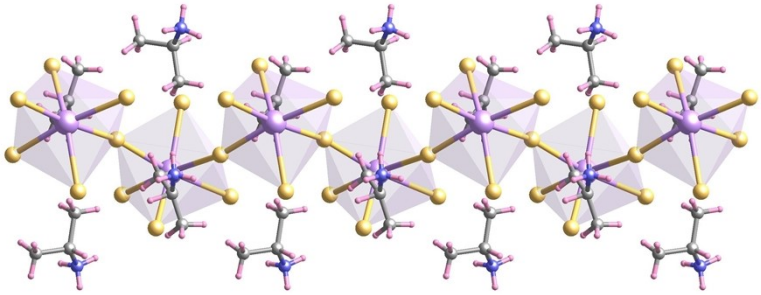

Fig. S6 Infinite 1D chain of $(C_3H_{10}N)_3PbBr_5$

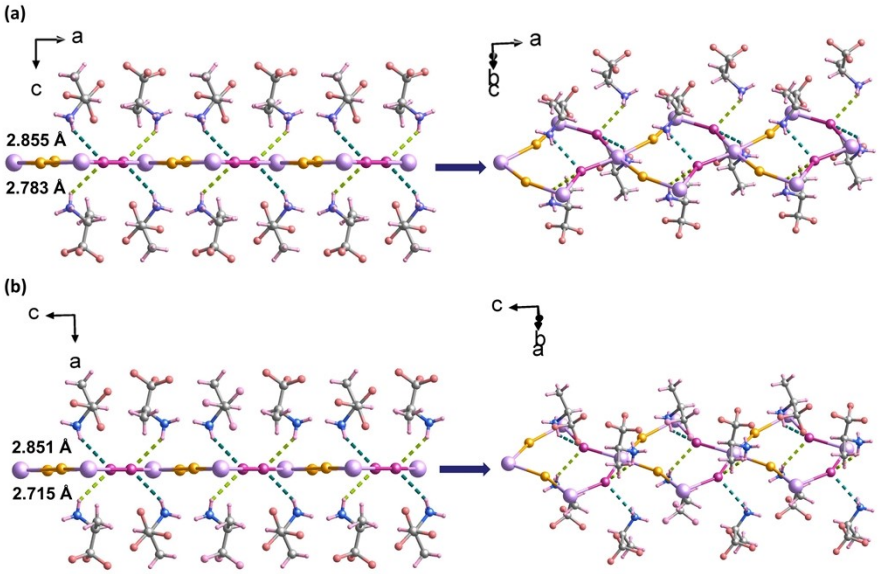

Fig. S7 Hydrogen-bonding interactions between the equatorial Br atoms and *R*-/*S*-$C_3H_7NF_3^+$ cations in (a) **1*R*** and (b) **2*S***.

The corresponding noncovalent H···Br (yellow-labelled) contacts exceed the van der Waals cutoff of 3.05 Å, meaning that the H···Br interactions are weak and negligible. The corresponding H···Br (purple-marked) distances about both sides of the inorganic layer are 2.855 Å, 2.783 Å for 1R, and 2.851 Å, 2.715 Å for 2S, respectively.

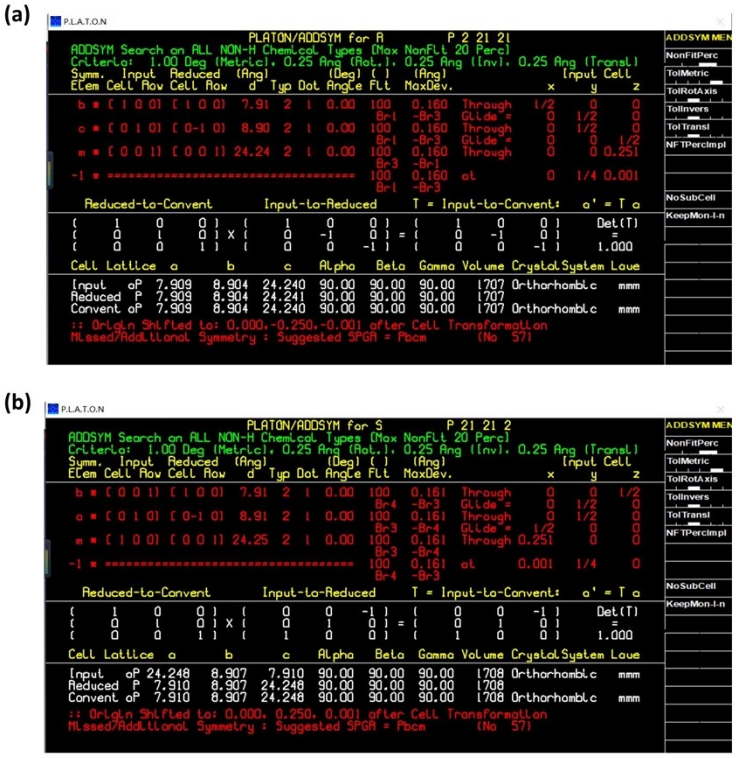

Fig. S8 Post-refinement analysis for missing symmetry using PLATON's ADDSYM tool on isolated inorganic frameworks (i.e., without organic cations) in (a) **1*R*** and (b) **2*S***. All the C, H, and N atoms were manually deleted from the fully refined structure using the CrystalMaker software.

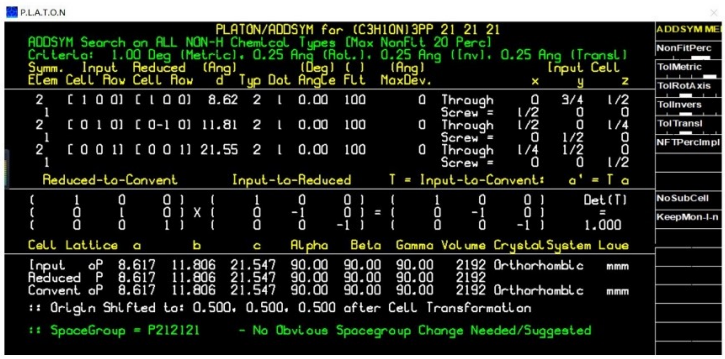

Fig. S9 Post-refinement analysis for missing symmetry using PLATON's ADDSYM tool on isolated inorganic frameworks (i.e., without organic cations) in $(C_3H_{10}N)_3PbBr_5$. All the C, H, and N atoms were manually deleted from the fully refined structure using the CrystalMaker software.

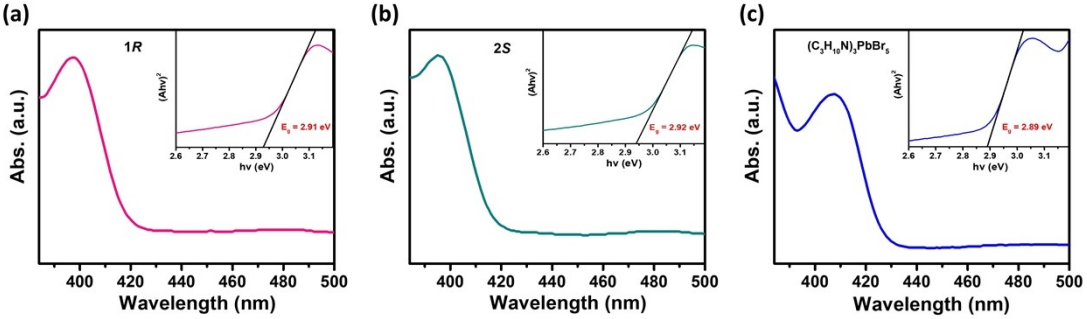

Fig. S10 Solid-state UV-visible absorption spectra of (a) **1*R***, (b) **2*S*** and (c) $(C_3H_{10}N)_3PbBr_5$ at room temperature. The insets show the band gaps of **1*R***/**2*S*** and $(C_3H_{10}N)_3PbBr_5$.

The optical bandgaps (E_g) of **1R**/**2S** were obtained from the Tauc plot equation $(h\nu\, F(R_\infty))^n = A(h\nu\, E_g)$ where h is Planck's constant, $F(R_\infty)$ is the Kubelka–Munk function, ν is the photon frequency, and A is the proportional constant. The bandgaps were estimated to be 2.91 (2.92) eV for **1R** (**2S**) and 2.89 eV for $(C_3H_{10}N)_3PbBr_5$.

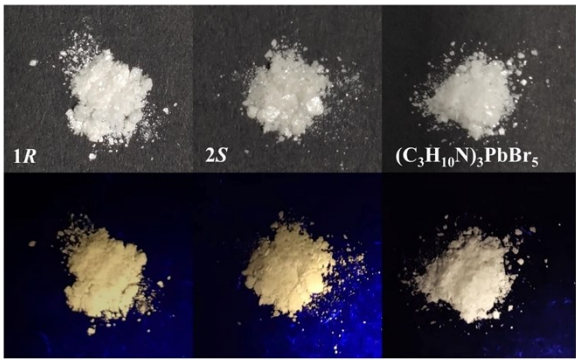

Fig. S11 The optical photos of **1*R***/**2*S*** and $(C_3H_{10}N)_3PbBr_5$ under natural (top) and ultraviolet light (bottom).

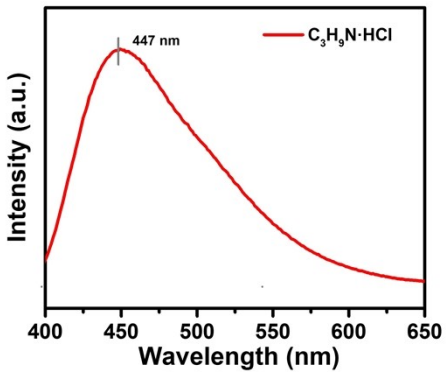

Fig. S12 The emission spectrum of chiral ligand salt $C_3H_9N{\cdot}HCl$.

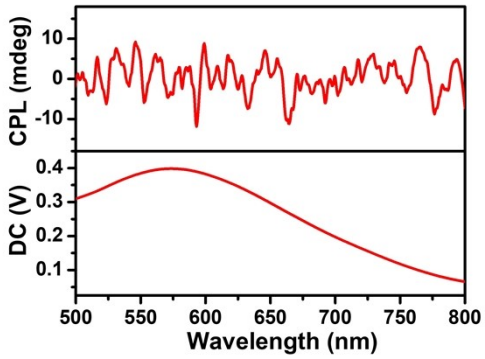

Fig. S13 CPL spectrum (top) of $(C_3H_{10}N)_3PbBr_5$ and the corresponding emission spectrum (bottom) in the solid state.

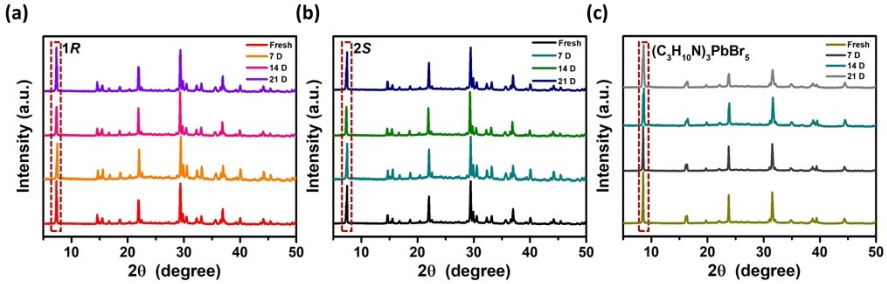

Fig. S14 PXRD patterns of (a) **1*R***, (b) **2*S*** and (c) $(C_3H_{10}N)_3PbBr_5$ after exposure to 75% humidity for 7, 14 and 21 Days.

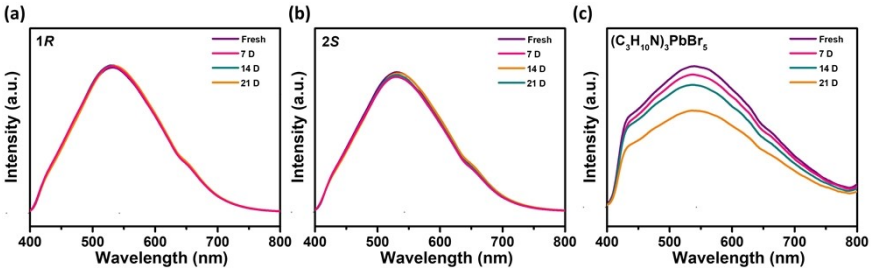

Fig. S15 The PL spectra of fresh (a) **1*R***, (b) **2*S*** and (c) $(C_3H_{10}N)_3PbBr_5$ after exposure to 75% humidity for 7, 14 and 21 Days.

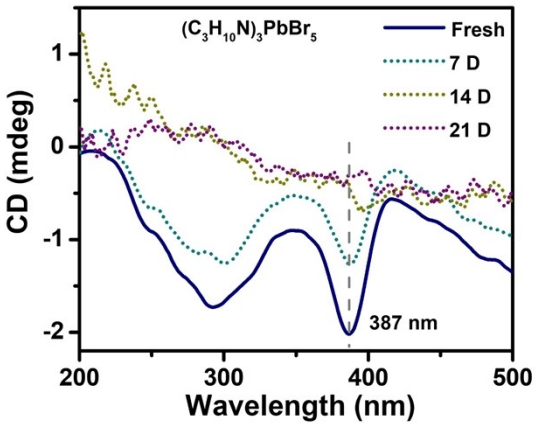

Fig. S16 The CD spectra of $(C_3H_{10}N)_3PbBr_5$ after exposure to 75% humidity for 7, 14 and 21 Days.

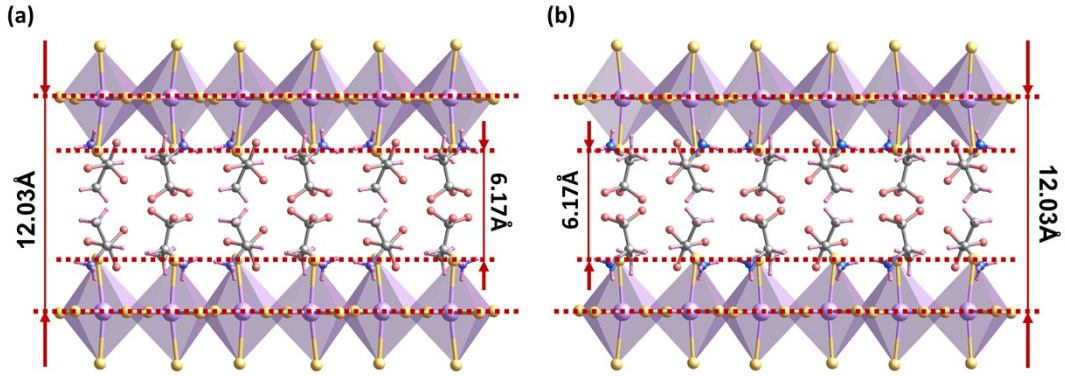

Fig. S17 The layer distances of (a) **1*R*** and (b) **2*S***.

Table S1. Crystal data and structure refinement for compound **1*R*** and **2*S***

	1*R*	**2*S***
Empirical formula	$C_6H_{14}Br_4F_6N_2Pb$	$C_6H_{14}Br_4F_6N_2Pb$
Formula weight	755.02	755.02
Temperature/K	199.99(10)	200.00(10)
Crystal system	orthorhombic	orthorhombic
Space group	$P22_12_1$	$P2_12_12$
a/Å	7.9087(2)	24.2480(2)
b/Å	8.9042(3)	8.90729(7)
c/Å	24.2405(8)	7.91028(7)
α/°	90	90
β/°	90	90
γ/°	90	90
Volume/Å^3	1707.03(9)	1708.49(3)
Z	4	4
ρ_{calc}g / cm^3	2.938	2.935
μ/mm^{-1}	30.669	30.643
F(000)	1360	1360
Crystal size/mm^3	0.03 × 0.02 × 0.02	0.03 × 0.02 × 0.02
Radiation	Cu Kα (λ = 1.54184)	Cu Kα (λ = 1.54184)
2θ range for data collection/°	7.294 to 147.568	10.58 to 147.482
Index ranges	-9 ≤ h ≤ 9, -6 ≤ k ≤ 10, -30 ≤ l ≤ 18	-30 ≤ h ≤ 30, -10 ≤ k ≤ 8, -9 ≤ l ≤ 9
Reflections collected	7425	15698
Independent reflections	3291 [R_{int} = 0.0724, R_{sigma} = 0.0840]	3382 [R_{int} = 0.0767, R_{sigma} = 0.0402]
Data/restraints/parameters	3291/0/176	3382/0/176
Goodness–of–fit on F^2	1.030	1.123
Final R indexes [I>=2σ (I)]	R_1 = 0.0592, wR_2 = 0.1555	R_1 = 0.0627, wR_2 = 0.1930
Final R indexes [all data]	R_1 = 0.0622, wR_2 = 0.1587	R_1 = 0.0636, wR_2 = 0.1944
Largest diff. peak/hole / e Å^{-3}	2.92/-2.62	6.42/-4.43
Flack parameter	0.00(2)	-0.001(11)
CCDC	2249682	2249985

$R_1 = \sum||F_o|-|F_c||/\sum|F_o|$. $wR_2 = [\sum w(F_o^2-F_c^2)^2/\sum w(F_o^2)^2]^{1/2}$

Table S2. Selected bond lengths (Å) for compound **1*R***

Bond lengths (Å)			
Pb1–Br2	3.177(17)	Pb1–Br1	2.946(2)
Pb1–Br2[1]	2.979(15)	Pb1–Br4	2.986(17)
Pb1–Br3	3.014(2)	Pb1–Br4[2]	3.118(15)

Symmetry codes: *[1]1-x, -1/2+y, 1/2-z; [2]-x, 1/2+y, 1/2-z; [3]1-x, 1/2+y, 1/2-z; [4]-x, -1/2+y, 1/2-z*

Table S3. Selected bond angles (°) for compound **1*R***

Bond angles (°)			
Br2[1]-Pb1-Br2	97.05(2)	Br1-Pb1-Br3	168.13(6)
Br2[1]-Pb1-Br3	98.70(5)	Br1-Pb1-Br4	89.48(5)
Br2[1]-Pb1-Br4	90.90(5)	Br1-Pb1-Br4[2]	85.25(6)
Br2[1]-Pb1-Br4[2]	173.06(5)	Br4-Pb1-Br2	172.05(5)
Br3-Pb1-Br2	87.70(5)	Br4[2]-Pb1-Br2	76.22(4)
Br1-Pb1-Br2[1]	82.89(6)	Br4-Pb1-Br3	91.18(6)
Br3-Pb1-Br2	93.14(5)	Br4-Pb1-Br4[2]	95.830(16)
Br1-Pb1-Br2	90.00(5)		

Symmetry codes:*1-x, -1/2+y, 1/2-z; [2]-x, 1/2+y, 1/2-z; [3]1-x, 1/2+y, 1/2-z; [4]-x, -1/2+y, 1/2-z*

Table S4. Selected bond lengths (Å) for compound **2*S***

Bond lengths (Å)			
Pb1–Br2[1]	2.980(17)	Pb1–Br4	3.016(2)
Pb1–Br2	3.180(17)	Pb1–Br5[2]	3.114(17)
Pb1–Br3	2.949(2)	Pb1–Br5	2.9923(18)

Symmetry codes: *[1]1/2-x, -1/2+y, 1-z; [2]1/2-x, 1/2+y,-z; [3]1/2-x, 1/2+y, 1-z; [4]1/2-x, -1/2+y, -z*

Table S5. Selected bond angles (°) for compound **2*S***

Bond angles (°)			
Br2[1]-Pb1-Br2	97.03(2)	Br3-Pb1-Br5[2]	85.25(5)
Br2[1]-Pb1-Br4	98.73(5)	Br4-Pb1-Br2	87.67(5)
Br2[1]-Pb1-Br5	90.88(5)	Br4-Pb1-Br5[2]	82.91(5
Br2[1]-Pb1-Br5[2]	173.06(5)	Br5[2]-Pb1-Br2	76.26(5)
Br3-Pb1-Br2[1]	93.08(5)	Br5-Pb1-Br2	172.09(5)
Br3-Pb1-Br2	89.99(5)	Br5-Pb1-Br4	91.20(5)
Br3-Pb1-Br4	168.15(6)	Br5-Pb1-Br5[2]	95.830(18)
Br3-Pb1-Br5	89.51(5)		

Symmetry codes *[1]1/2-x, -1/2+y, 1-z; [2]1/2-x, 1/2+y, -z; [3]1/2-x, 1/2+y, 1-z; [4]1/2-x, -1/2+y, -z*

Table S6. Parameters of the hydrogen bonds in compound **1*R***

D-H	d(D-H) (Å)	d(H..A) (Å)	<DHA (°)	d(D..A) (Å)	A
N1-H1A	0.910	2.554	152.68	3.388	BR3
N1-H1B	0.910	2.774	126.30	3.393	BR2
N1-H1B	0.910	3.048	110.82	3.477	BR5
N1-H1C	0.910	2.391	177.93	3.301	BR4
N3-H3A	0.910	2.858	117.35	3.374	BR2
N3-H3B	0.910	2.458	162.84	3.338	BR4
N3-H3C	0.910	2.429	155.42	3.279	BR3
C13-H13A	0.980	2.639	120.11	3.244	F7
C13-H13C	0.980	3.011	137.55	3.792	BR3
C15-H15A	0.980	3.041	114.65	3.563	BR4
C15-H15B	0.980	2.980	136.36	3.750	BR3
C15-H15C	0.980	3.056	147.77	3.920	BR5

Symmetry codes: *-x, y+1/2, -z+1/2; -x, -y+5/2, z+1/2; x, y+1, z; -x+1, y+1/2, -z+1/2.*

Table S7. Parameters of the hydrogen bonds in compound **2*S***

D-H	d(D-H) (Å)	d(H..A) (Å)	<DHA (°)	d(D..A) (Å)	A
N1-H1A	0.910	2.706	135.63	3.417	BR2
N1-H1A	0.910	3.045	112.50	3.495	BR5
N1-H1B	0.910	2.489	163.18	3.371	BR4
N1-H1C	0.910	2.424	168.12	3.320	BR3
C8-H8A	0.980	2.614	122.16	3.243	F10
C8-H8B	0.980	2.982	138.17	3.769	BR4
N9-H9A	0.910	2.425	156.23	3.278	BR4
N9-H9B	0.910	2.453	164.67	3.339	BR3
N9-H9C	0.910	2.835	118.73	3.368	BR2
C10-H10B	0.980	3.048	128.37	3.736	BR4
C10-H10C	0.980	3.048	115.16	3.576	BR3

Symmetry codes: *-x+1/2, y-1/2, -z; x-1/2, -y+1/2, -z; x, y, z-1; -x+1/2, y+1/2, -z.*

Table S8. Crystal data and structure refinement for compound $(C_3H_{10}N)_3PbBr_5$

	$(C_3H_{10}N)_3PbBr_5$
Empirical formula	$C_9H_{30}Br_5N_3Pb$
Formula weight	787.10
Temperature/K	200.00(10)
Crystal system	orthorhombic
Space group	$P2_12_12_1$
a/Å	8.6172(3)
b/Å	11.8062(5)
c/Å	21.5472(9)
α/°	90

β/°	90
γ/°	90
Volume/Å^3	2192.13(15)
Z	4
ρ_{calc}g / cm^3	2.385
μ/mm^{-1}	16.802
F(000)	1448
Crystal size/mm^3	0.03 × 0.02 × 0.02
Radiation	Mo Kα (λ = 0.71073)
2θ range for data collection/°	3.78 to 57.748
Index ranges	-11 ≤ h ≤ 9, -12 ≤ k ≤ 16, -23 ≤ l ≤ 28
Reflections collected	12421
Independent reflections	4853 [R_{int} = 0.0357, R_{sigma} = 0.0531]
Data/restraints/parameters	4853/34/181
Goodness–of–fit on F^2	1.160
Final R indexes [I>=2σ (I)]	R_1 = 0.0353, wR_2 = 0.0890
Final R indexes [all data]	R_1 = 0.0470, wR_2 = 0.1142
Largest diff. peak/hole / e Å^{-3}	1.35/-2.15
Flack parameter	-0.014(7)
CCDC	2249681

$R_1 = \sum||F_o|-|F_c||/\sum|F_o|$. $wR_2 = [\sum w(F_o^2-F_c^2)^2/\sum w(F_o^2)^2]^{1/2}$

Table S9. Selected bond lengths (Å) for compound $(C_3H_{10}N)_3PbBr_5$

Bond lengths (Å)			
Pb1–Br5	3.048(15)	Pb1–Br2	2.935(16)
Pb1–Br3[1]	3.103(14)	Pb1–Br4	3.098(17)
Pb1–Br3	3.005(14)	Pb1–Br1	2.912(17)

Symmetry codes: *[1]1/2+x, 3/2-y, 1-z; [2]-1/2+x, 3/2-y, 1-z.*

Table S10. Selected bond angles (°) for compound $(C_3H_{10}N)_3PbBr_5$

Bond angles (°)			
Br5-Pb1-Br3[1]	81.89(4)	Br2-Pb1-Br3	85.50 (4)
Br5-Pb1-Br4	91.56(5)	Br2-Pb1-Br3[1]	85.21(4)
Br3-Pb1-Br5	172.18(4)	Br2-Pb1-Br4	164.84(5)
Br3-Pb1-Br3[1]	92.422(15)	Br4-Pb1-Br3[1]	85.90(4)
Br3-Pb1-Br4	82.63(4)	Br1-Pb1-Br5	98.58(5)

Br2-Pb1-Br5	99.30(4)	Br1-Pb1-Br3	87.71(5)
Br1-Pb1-Br3[1]	173.19(5)	Br1-Pb1-Br4	100.87(5)
Br1-Pb1-Br2	88.01(5)		

Symmetry codes *[1]1/2+x, 3/2-y ,1-z; [2]-1/2+x, 3/2-y, 1-z.*

Table S11. Parameters of the hydrogen bonds in compound $(C_3H_{10}N)_3PbBr_5$

D-H	d(D-H) (Å)	d(H..A) (Å)	<DHA (°)	d(D..A) (Å)	A
C3-H3A	0.980	3.037	111.43	3.516	BR3
C3-H3B	0.980	3.057	119.27	3.638	BR3
C3-H3C	0.980	2.556	168.71	3.523	BR5
C8-H8B	0.980	2.597	159.56	3.532	BR2
C8-H8A	0.980	2.568	160.05	3.505	BR3
C4-H4A	0.980	2.384	162.22	3.331	BR4
C4-H4B	0.980	2.554	134.99	3.320	BR5
C4-H4C	0.980	2.415	166.80	3.376	BR1
C1-H1F	0.980	3.053	132.91	3.789	BR2
C7-H7A	0.980	3.132	139.05	3.925	BR2
C6-H6C	0.980	3.063	150.46	3.945	BR5
C9-H9A	1.00	2.964	132.23	3.711	BR4

Symmetry codes: *x-1/2, -y+3/2, -z+1; x-1, y, z; x+1/2, -y+3/2, -z+1; x+1, y, z; -x+1, y+1/2, -z+1/2;*

References

[1] CrysAlisPro **2012**, Agilent Technologies. Version 1.171.36.31.

[2] Sheldrick, G. M. Acta Crystallogr. *Sect. A* **2015**, *71*, 3-8.

[3] Dolomanov, O. V.; Bourhis, L. J.; Gildea, R. J.; Howard, J. A. K.; Puschmann, H. OLEX2: A Complete Structure Solution, Refinement and Analysis Program. *J. Appl. Cryst*. **2009**, *42*, 339-341.

[4] Sheldrick, G. M. Crystal Structure Refinement with SHELXL. *Acta Cryst*. *C* **2015**, *71*, 3-8.

[5] Kresse, G.; Hafner, J. Ab Initio Molecular Dynamics for Open-Shell Transition Metals *Phy. Rev*. *B* **1993**, *48*, 13115−13118.

[6] Kresse, G.; Furthmüller, J. Efficient Iterative Schemes for Ab Initio Total-Energy Calculations Using a Plane-wave Basis Set. *Phy. Rev. B* **1996**, *54*, 11169−11186.

[7] Perdew, J. P.; Burke, K.; Ernzerhof, M. Generalized Gradient Approximation Made Simple. *Phys. Rev*. *Lett*. **1996**, *77*, 3865–3868.

[8] Grimme, S.; Antony, J.; Ehrlich, S.; Krieg, H. A Consistent and Accurate Ab Initio Parametrization of Density Functional Dispersion Correction (DFT-D) for the 94 Elements H-Pu. *J. Chem. Phys.* **2010**, *132*, 154104.

[9] Grimme, S., Wiley Interdiscip. *Rev. Mol. Sci*. **2011**, *1*, 211−228.